

The Fourier heat conduction as a strong kinetic effect

Hanqing Zhao^{1,2} and Wen-ge Wang¹

¹Department of Modern Physics, University of Science and Technology of China, Hefei 230026, China

²School of Physical Science and Technology, and Key Laboratory for Magnetism and Magnetic Materials of MOE, Lanzhou University, Lanzhou, Gansu 730000, China

For an one-dimensional (1D) momentum conserving system, intensive studies have shown that generally its heat current autocorrelation function (HCAF) tends to decay in a power-law manner and results in the breakdown of the Fourier heat conduction law in the thermodynamic limit. This has been recognized to be a dominant hydrodynamic effect. Here we show that, instead, the kinetic effect can be dominant in some cases and leads to the Fourier law. Usually the HCAF undergoes a fast decaying kinetic stage followed by a long, slowly decaying hydrodynamic tail. In a finite range of the system size, we find that whether the system follows the Fourier law depends on whether the kinetic stage dominates. Our study is illustrated by the 1D diatomic gas model, with which the HCAF is derived analytically and verified numerically by molecular dynamics simulations.

Driven by applications of nanomaterials, heat conduction properties of low-dimension materials have been a focus topic in the past three decades [1–7]. Based on numerous theoretical studies, it is concluded that in general, the thermal conductivity of a low-dimensional momentum conserving system has a system-size dependent abnormality in the thermodynamic limit [8–10]. This abnormality is attributed to the hydrodynamic effect that induces the slow power-law decay of the heat current autocorrelation function (HCAF) [8, 9]. However, counterexamples, i.e., momentum conserving systems but yet having a size-independent thermal conductivity, have been found [10–13]. These counterexamples usually have asymmetric interparticle interactions, including the Toda-like models [12], Lennard-Jones model [10, 11, 13], the Fermi-Pasta-Ulam- α - β model [14], the diatomic gas model [15, 16], the diatomic Toda model [16], and so on. More importantly, so far direct experimental measurements have not provided solid evidence yet to support the predicted abnormality in real low-dimensional materials of finite sizes available.

In one dimensional (1D) case, the heat conductivity, denoted by κ , is related to the HCAF, denoted by $C(t)$, by the Green-Kubo formula

$$\kappa = \lim_{t_c \rightarrow \infty} \lim_{L \rightarrow \infty} \frac{1}{k_B T^2 L} \int_0^{t_c} C(t) dt. \quad (1)$$

Here k_B is the Boltzmann constant, L and T are, respectively, the size and the temperature of the system, and $C(t) \equiv \langle J(0)J(t) \rangle$, with $J(t)$ being the total heat current at time t and $\langle \cdot \rangle$ representing the equilibrium ensemble average. For a finite system, Lepri *et al.* [3] suggest to drop the limits and truncate the integral at $t_c = L/c_s$ (c_s is the sound speed) to calculate the heat conductivity [3, 10]. It leads to $\kappa \sim L^{1-\alpha}$ in the thermodynamical limit given that $C(t)$ tends to decay as $\sim t^{-\alpha}$ as $L \rightarrow \infty$.

In trying to understand the aforementioned counterexamples and the existing experimental results, Chen *et al.* conjectured that the asymmetric interactions may practically lead to a size-independent thermal conductivity in a certain finite system size range [10], because the hydrodynamic approach may not apply to systems of asymmetric interactions in a transient, but may be long time period.

In this transient period, the HCAF may decay faster, but its contribution to the thermal conductivity can dominate until that contributed by the hydrodynamic power-law tail becomes comparable after a sufficient long time. Therefore, though the predicted abnormality can be the case in the thermodynamics limit, normal heat conduction following the Fourier law can still be expected in a finite system size range. This would have significant practical implications because any real materials are in fact finite.

It is thus important to establish a complete theory based on which the kinetic effect can be evaluated and taken into account as well. This is our motivation and in this work, we will focus on the 1D diatomic gas [17], a paradigmatic, momentum conserving fluid model. The hard-core elastic collision occurring when two neighboring particles meet can be considered as an effective asymmetric interaction. It is worth noting that there has been a long-term argumentation towards the heat conduction property of this model. In 2001, Garrido *et al.* presented the numerical evidence to show that this model has a convergent thermal conductivity in the thermodynamic limit [18]. This result was questioned by many other authors [19–21] because of the clear power-law decaying tail in the HCAF. Nevertheless, a recent numerical study showed that interestingly, when the two types of particles in the system have close masses, the heat conductivity does not depend on the system size in a certain system size range [16]. Moreover, it is observed that the HCAF shows an exponential-like decay in a transient stage, and the time this transient stage lasts increases rapidly as the mass ratio tends to 1. Therefore, the mass ratio is a key parameter for the heat conduction property of this model. In view of the subtlety of this issue and the limitation of the numerical simulations, an analytical study is particularly desired. In the following we will show that the idea of the conventional kinetic approach can be borrowed for our aim here.

First of all, suppose that our model consists of N particles with alternative masses μ_1 and μ_2 queueing on a line. We assume that $\mu_1 > \mu_2$ and define $r = \mu_1/\mu_2$ as the mass ratio. Let m_i and v_i be the mass and velocity of the i th particle; after a collision, the velocities of the

two neighboring particles, say the i th and the $(i+1)$ th, change into

$$\begin{aligned} v_i(t+1) &= \frac{m_i - m_{i+1}}{m_i + m_{i+1}} v_i(t) + \frac{2m_{i+1}}{m_i + m_{i+1}} v_{i+1}(t), \\ v_{i+1}(t+1) &= \frac{m_{i+1} - m_i}{m_i + m_{i+1}} v_{i+1}(t) + \frac{2m_i}{m_i + m_{i+1}} v_i(t), \end{aligned} \quad (2)$$

where the time t is measured as the number of collisions. Note that this dynamics keeps the total momentum and energy of the system.

In the kinetic theory, for characterizing the Brownian motion, one traces a tagged particle and studies the decay of its velocity autocorrelation function. In our model a particle is always bounded by its two neighbors. Hence, instead tracing a tag particle, we record the energy the tagged particle carries initially, which we term as the ‘tagged energy’, and investigate how it spreads over the system. Note that during a collision, the energy carried by a particle will separate into two parts; one part remains on itself, while another part transfers to the other particle. If the two particles have close masses, then the transferred part will hold a large proportion. For the sake of convenience, in the following we term this transferred part of energy as the dominant energy since it dominates the decay behavior of the HCAF before the hydrodynamic process takes over. Similarly, we term the particle that carries the dominant energy as the dominant carrier. (At a given time there is only one dominant carrier.) Then the tagged energy can be traced by following the ensuing dominant energy sequence and in turn by tracing the dominant carriers. This is the key technique we adopt for our analytical treatment, which can be seen as an extension of the conventional kinetic approach.

As an example, let us take the i th particle as the tagged particle and assume its first collision happens with the $(i+1)$ th particle. According to Eq. (2), after the collision its initial velocity $v_i(0)$ separates into two parts, the remaining part $\frac{m_i - m_{i+1}}{m_i + m_{i+1}} v_i(0)$ and the transferred part $\frac{2m_{i+1}}{m_i + m_{i+1}} v_i(0)$. For $m_1 \approx m_2$, the remaining part will be much smaller than the transferred, the $(i+1)$ th particle thus carries the dominant energy and becomes the dominant carrier. As the velocity component $\frac{2m_{i+1}}{m_i + m_{i+1}} v_i(0)$ in $v_{i+1}(1)$ comes from $v_i(0)$, it correlates with $v_i(0)$. Similarly, when the next collision happens between the $(i+1)$ th particle and one of its neighbors (no matter the i th or the $(i+2)$ th as they have the same masses), the transferred velocity that contains $v_i(0)$ is $\frac{4m_i m_{i+1}}{(m_i + m_{i+1})^2} v_i(0) = \frac{4r}{(1+r)^2} v_i(0)$. It is thus straightforward that after $2P$ collisions, the portion of $v_i(0)$ that transferred to the dominant carrier is

$$v_i(0) \left[\frac{4m_i m_{i+1}}{(m_i + m_{i+1})^2} \right]^P = v_i(0) \left[\frac{4r}{(1+r)^2} \right]^P. \quad (3)$$

Now let us consider the HCAF. The total energy current is defined as $J(t) \equiv \sum_q^N j_q(t)$, where $j_q(t) \equiv \frac{1}{2} m_q v_q^3(t)$ is the local current on the q th particle. Still

taking the i th particle as the tagged particle, we have [3, 12]

$$\langle J(t) J(0) \rangle = N \sum_q^N \langle j_q(t) j_i(0) \rangle, \quad (4)$$

Suppose that at time $t = 2P$ the the dominate carrier is the k th particle and t_F is the average time for the dominant energy transferring from one dominant carrier to the next; For $r \rightarrow 1$, we have $j_q(t) j_i(0) \neq 0$ for $q = k$ and other $j_q(t) j_i(0)$ terms are negligible. This gives that

$$C(t) = N \left[\frac{64r^3}{(r+1)^6} \right]^{\frac{t}{2t_F}} \langle j_i(0) j_k(0) \rangle, \quad (5)$$

which can be rewritten as

$$\langle C(t) \rangle = \langle C(0) \rangle e^{-\frac{t}{\tau}} \quad (6)$$

with

$$\tau = -2t_F \left[\ln \left(\frac{64r^3}{(r+1)^6} \right) \right]^{-1}. \quad (7)$$

Equations (6) and (7) are our main result, which indicate that the HCAF decays exponentially in the kinetic stage. The physics picture behind Eq. (6) is indeed similar to that of the Brownian motion. In our case, the tagged particle is bounded, but its energy is dispersed due to the interactions with and among the surrounding particles, resulting in an exponentially decaying energy current autocorrelation function. In our model, the dominant carrier changes from one to another. During this process, the tagged energy keeps losing, so that the HCAF, dominated by remained energy from dominant carriers, decays exponentially. Therefore, our treatment is the same in spirit as the conventional kinetic approach. The parameter to be determined is t_F . As it is generally accepted that the energy is transported by the sound modes [22], it is reasonable to assume that the energy is transferred at the sound speed as well, and therefore we have $t_F = \frac{a}{c_s}$, where a is the average distance between two neighboring particles. (Throughout this work we set $a = 1$ so that $N = L$.)

By substituting (6) into the Green-Kubo formula (1), we can obtain the thermal conductivity due to the kinetic effect exclusively:

$$\kappa_k = \frac{\tau}{k_B T^2} C(0). \quad (8)$$

When the hydrodynamic contribution is negligible in a finite system, we have $\kappa \approx \kappa_k$. In fact, as the dominant energy keeps losing [see Eq. (3)], the energy transferred to other particles can not be neglected after a sufficient long time. This part of energy evolves following the hydrodynamics and can be captured by the hydrodynamics approaches [9]. The decaying behavior of the HCAF induced by the hydrodynamics process has been worked out [8, 9, 23], which reads $C_H(t) = ct^{-\frac{2}{3}}$ in the thermodynamic limit. The parameter c is the amplitude of

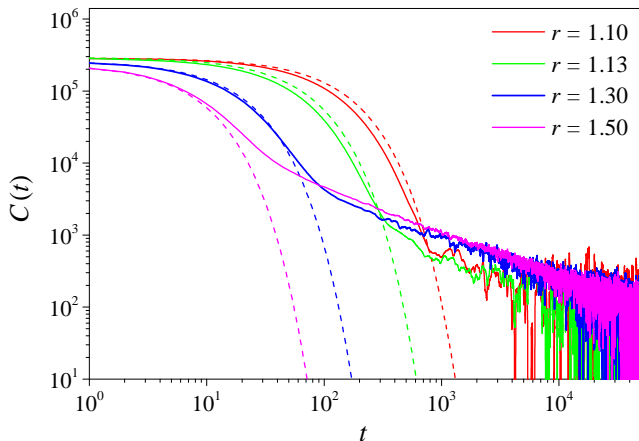


FIG. 1: The heat current autocorrelation function of the 1D diatomic gas model at various mass ratios. The solid lines are for simulation results and the dashed lines of the same color are for the corresponding analytical predictions [Eq. (6)] based on our extended kinetic theory. In simulations, the system size is set to be $N = 50000$. Here and in all other figures, $k_B = 1$, $T = 1$ and $\mu_2 = 1$.

the power-law tail. Roughly, we can identify the time, denoted by t_1 , that separates the kinetic and the hydrodynamic stage by the condition

$$C(0)e^{-\frac{t_1}{\tau}} = ct_1^{-\frac{2}{3}}. \quad (9)$$

For $t < t_1$, the kinetic effect dominates. Because as $r \rightarrow 1$, both τ and t_1 increase [see Eq. (7) and (13)], the kinetic region can last so long to allow the HCAF to decay for orders in the amplitude (see Fig. 1 for $r = 1.1$ as an example). On the other hand, for $t > t_1$, the hydrodynamic effect begins to take over, but its contribution to the heat conductivity will not be comparable before another time scale, denoted by t_2 , that can be estimated by

$$\kappa_H = c \int_{t_1}^{t_2} t^{\frac{2}{3}} dt. \quad (10)$$

Namely, for $t > t_2$, we have $\kappa_H > \kappa_k$. The time scale t_1 and t_2 thus suggest two characteristic system sizes $L_1 = c_s t_1$ and $L_2 = c_s t_2$, for $L_1 < L < L_2$ we can expect that the heat conductivity is in effect independent of the system size. This is consistent with the previous numerical study [16] (see also Fig. 2 for $r = 1.1$ as an example).

Our method can be adopted to study other 1D gas models. An immediate application is to the model with periodically repeating unit of one heavy particle of mass μ_1 and $Z - 1$ light particles of mass μ_2 . In this model, when two light particles collide, they simply exchange their velocities. Hence the dominant energy is transferred along the $Z - 1$ light particles ballistically without any decay till the collision with a heavy particle occurs. As a result, the time t_F should be $Z - 1$ times of that in

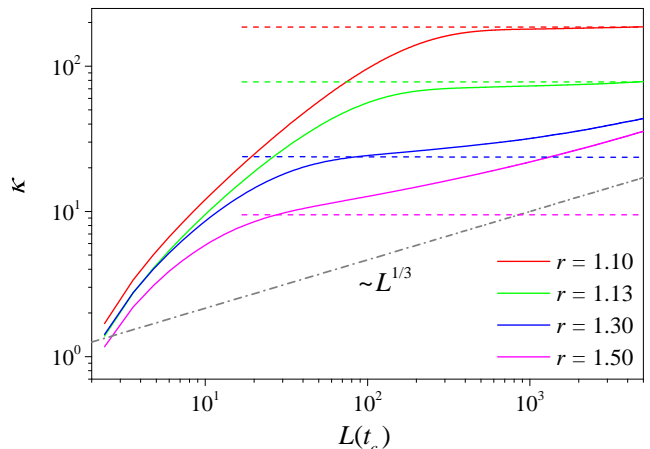


FIG. 2: The heat conductivity of the 1D diatomic gas model as a function of the system size at various mass ratios. The solid lines are for the results based on the Green-Kubo formula by integrating the heat current autocorrelation function numerically obtained. The horizontal dashed lines of the same color are for the corresponding result κ_k [Eq. (8)] due to the pure kinetic effect.

the alternative diatomic gas, i.e., $t_F = \frac{(Z-1)a}{c_s}$. Hence Eq. (6) and (7) do not change except that the value of t_F in (7) should be replaced.

Our method can be applied to models with random masses as well. Let us first consider the random diatomic gas model, where a particle has a probability of $1/2$ to adjoin the same type of particles. The isotactic clusters formed have an average length of $\langle b \rangle = \sum_{i=0}^{+\infty} \frac{1}{2}^i a = 2a$, which implies that on average $t_F = \frac{2a}{c_s}$. So again we only need replace the value of t_F in Eq. (7). For the more general model where all the particles have random but close masses, on average after a collision the HCAF is

$$\langle J(t_F)J(0) \rangle = 8 \left\langle \frac{m_i^2 m_{i+1}}{(m_i + m_{i+1})^3} \right\rangle C(0), \quad (11)$$

where $\left\langle \frac{m_i^2 m_{i+1}}{(m_i + m_{i+1})^3} \right\rangle$ is determined by the mass distribution. After time t the dominant carrier experienced P collision, and $t = P t_F$. The HCAF in the transient kinetic process also follows Eq. (6) and (7) with

$$\tau = -t_F \left[\ln \left(\frac{m_i^2 m_{i+1}}{(m_i + m_{i+1})^3} \right) \right]^{-1}. \quad (12)$$

Now we put our analytical results into numerical check with the 1D diatomic gas model. As how to calculate analytically the sound speed of this model is still an open problem, we evaluate the sound speed by the aid of numerical simulations as well [14, 24, 25]. (Note that recently the sound speed for nonlinear 1D lattices with analytical interactions has been derived analytically [8]. It, however, does not apply to the 1D gas models.) In doing so, we measure the sound speed by tracing the motion of the sound mode peaks in the spatio-temporal correlation function of the heat current density fluctuations [25]

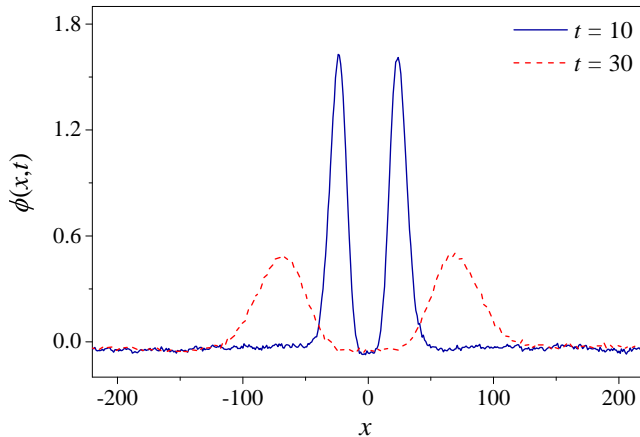


FIG. 3: The numerical simulation results of the spatio-temporal correlation functions of heat current density fluctuations of the 1D diatomic model with $r = 1.3$ at $t = 10$ (blue line) and $t = 30$ (red line) respectively. By tracing the sound mode peaks the sound speed is measured numerically.

(see. Fig. 3). For $1.1 \leq r \leq 1.5$, we find that $c_s \approx 2.3$. For the HCAF, in our simulations a system consisting of 50000 particles with periodic boundary condition is considered. The numerical results and the analytical results are compared in Fig. 1 for various mass ratios. We can see that the predicted HCAF based on the kinetic effect agrees with the simulation result very well in the transient time region $t < t_1$. In Fig. 2 we plot the corresponding thermal conductivity calculated by the Green-Kubo formula as a function of the system size, where, for a given system size L , κ is measured by integrating $C(t)$ up to the truncated time $t_c = L/c_s$. It shows that the kinetic approach does allow us to predict the system-size independent range of κ , which increases as $r \rightarrow 1$. For larger r this range disappears though a crossover can be identified. The prediction fails for larger r since the hydrodynamic effect begins to play a significant role before the HCAF decays to a sufficient small value. For example, for $r = 1.3$, the hydrodynamic contribution becomes dominant rapidly and the power-law divergence of $\kappa \sim L^{\frac{1}{3}}$ can be recognized for $t > 10^3$ (see. Fig. 2).

Next, we check the time scale t_1 . To evaluate it by Eq. (9), we need to know the parameter c in principle. However, the hydrodynamic approach has not solved it yet. (Note that the analytical approach developed by Spohn [8] applies only to the 1D lattices with analytical interactions.) Fortunately, we notice that t_1 does not depend on c sensitively. In fact, Eq. (9) can be rewritten as $\frac{t_1}{\tau} + \ln\left(\frac{c}{\langle C(0) \rangle}\right) = \frac{2}{3} \ln(t_1)$. As for $r \rightarrow 1$, t_1 is large, while the term $\ln\left(\frac{c}{\langle C(0) \rangle}\right)$ is negligible since $\frac{c}{\langle C(0) \rangle} \sim 10^{-1}$ [23], we therefore can solve the following equation

$$\frac{t_1}{\ln(t_1)} = \frac{2}{3}\tau \quad (13)$$

to estimate t_1 . The result is shown in Fig. 4. One can see that it agrees very well with that obtained by simulations.

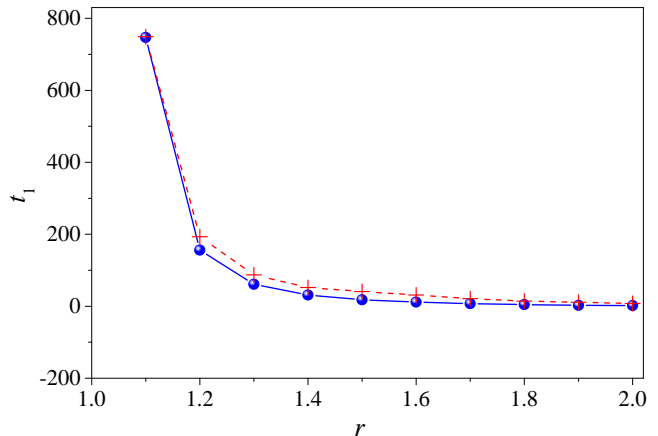


FIG. 4: Comparison of the time scale t_1 in the 1D diatomic gas model that separates the kinetic and hydrodynamic processes obtained by Eq. (9) analytically (red crisscrosses) and by simulations (blue bullets).

(In simulations, t_1 is identified to be the convex-concave transition point of the HCAF.) From Fig. 4, it is seen that for $r > 1.5$, t_1 drops to the order of 1, suggesting that the hydrodynamic region covers almost the entire time region. This is also consistent with previous numerical studies that claimed the abnormal heat conduction with $r > 1.5$.

Finally we present the results for variant 1D diatomic gas models. In Fig. 5(a)-(c), we compare the analytically predicted and simulated HCAF's for, respectively, the periodic model with repeating unit of $\mu_1 - \mu_2 - \mu_2$, the random diatom model with binary isotactic clusters of μ_1 and μ_2 , and the random mass model with uniformly distributed masses $m_i \in (1, 1.4)$. In all three cases, the analytical results fit the simulation results very well in the kinetic region $t < t_1$.

In summary, by introducing and tracing the tagged energy, we extend the kinetic approach to characterize the HCAF in the time region where the kinetic effect dominates. The system-size independent heat conductivity observed in previous studies, including its value and the system size range, is predicted quantitatively. Our study indicates that a full description of the HCAF should incorporate both the kinetic and hydrodynamic effects. Our method may be applicable to other momentum conserving systems.

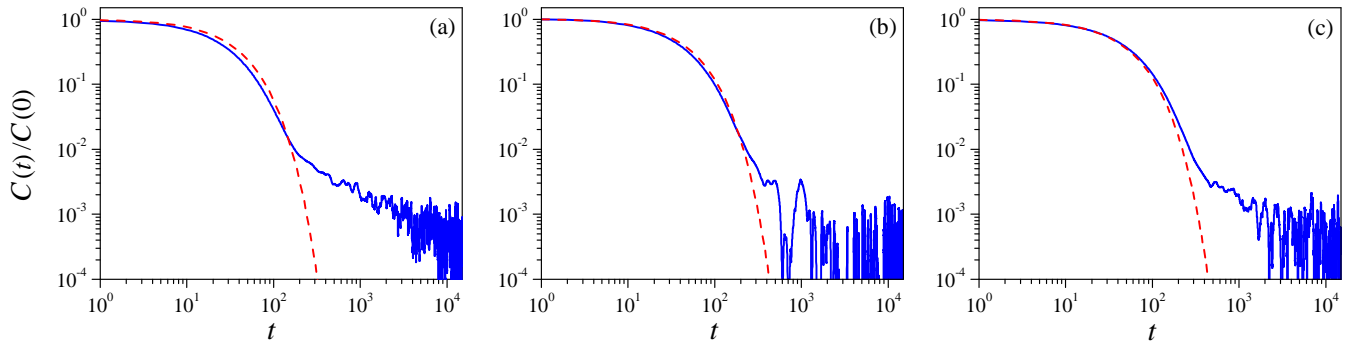


FIG. 5: The heat current autocorrelation function for three variant 1D gas models. (a) Periodic diatom model with repeating $\mu_1 - \mu_2 - \mu_2$ unit. (b) Random diatomic gas model. In (a) and (b), $\mu_1 = 1.2$ and $\mu_2 = 1$. (c) Random gas model with the particle masses uniformly distributed between 1 and 1.4. In all the panels, the red dashed line is for the theoretical prediction given by Eq. (6) and the black solid line is for the simulation result.

-
- [1] M. Y. Han, J. C. Brant, and P. Kim. Electron transport in disordered graphene nanoribbons. *Phys. Rev. Lett.*, 104:056801, Feb 2010.
- [2] A. M. Marconnet, M. A. Panzer, and K. E. Goodson. Thermal conduction phenomena in carbon nanotubes and related nanostructured materials. *Rev. Mod. Phys.*, 85:1295–1326, Aug 2013.
- [3] S. Lepri, R. Livi, and A. Politi. Thermal conduction in classical low-dimensional lattices. *Phys. Rep.*, 377(1):1–80, 2003.
- [4] A. Dhar. Heat transport in low-dimensional systems. *Adv. Phys.*, 57(5):457–537, 2008.
- [5] N. Li, J. Ren, L. Wang, G. Zhang, P. Hänggi, and B. Li. Colloquium: Phononics: Manipulating heat flow with electronic analogs and beyond. *Rev. Mod. Phys.*, 84(3):1045, 2012.
- [6] F. Bonetto, J. L. Lebowitz, and L. Rey-Bellet. *Fourier’s law: A challenge for theorists*. 2000.
- [7] J. Wang and G. Casati. One-dimensional self-organization and nonequilibrium phase transition in a hamiltonian system. *Phys. Rev. Lett.*, 118(4):040601, 2017.
- [8] C. B. Mendl and H. Spohn. Dynamic correlators of fermi-pasta-ulam chains and nonlinear fluctuating hydrodynamics. *Phys. Rev. Lett.*, 111:230601, Dec 2013.
- [9] H. van Beijeren. Exact results for anomalous transport in one-dimensional hamiltonian systems. *Phys. Rev. Lett.*, 108:180601, Apr 2012.
- [10] S. Chen, Y. Zhang, J. Wang, and H. Zhao. Key role of asymmetric interactions in low-dimensional heat transport. *J. Stat. Mech.*, (3):033205, 2016.
- [11] S. Chen, Y. Zhang, J. Wang, and H. Zhao. Breakdown of the power-law decay prediction of the heat current correlation in one-dimensional momentum conserving lattices. *arXiv:1204.5933*, 2012.
- [12] Y. Zhong, Y. Zhang, J. Wang, and H. Zhao. Normal thermal conduction in lattice models with asymmetric harmonic interparticle interactions. *Chinese Physics B*, 22(7):70505, 2013.
- [13] A. V. Savin and Y. A. Kosevich. Thermal conductivity of molecular chains with asymmetric potentials of pair interactions. *Phys. Rev. E*, 89(3):032102, 2014.
- [14] S. G. Das, A. Dhar, K. Saito, C. B. Mendl, and H. Spohn. Numerical test of hydrodynamic fluctuation theory in the fermi-pasta-ulam chain. *Phys. Rev. E*, 90:012124, Jul 2014.
- [15] S. Chen, Y. Zhang, J. Wang, and H. Zhao. Finite-size effects on current correlation functions. *Phys. Rev. E*, 89:022111, Feb 2014.
- [16] S. Chen, J. Wang, G. Casati, and G. Benenti. Nonintegrability and the fourier heat conduction law. *Phys. Rev. E*, 90:032134, Sep 2014.
- [17] G. Casati. Energy transport and the fourier heat law in classical systems. *Found. Phys.*, 16(1):51–61, 1986.
- [18] P. L. Garrido, P. I. Hurtado, and B. Nadrowski. Simple one-dimensional model of heat conduction which obeys fourier’s law. *Phys. Rev. Lett.*, 86:5486–5489, Jun 2001.
- [19] A. Dhar. Comment on “simple one-dimensional model of heat conduction which obeys fourier’s law”. *Phys. Rev. Lett.*, 88:249401, Jun 2002.
- [20] H. Li, Y. Wang, and H. Zhao. Comment on “simple one-dimensional model of heat conduction which obeys fourier’s law”. *Phys. Rev. Lett.*, 89:079401, Jul 2002.
- [21] P. Grassberger, W. Nadler, and L. Yang. Heat conduction and entropy production in a one-dimensional hard-particle gas. *Phys. Rev. Lett.*, 89:180601, Oct 2002.
- [22] J. P. Hansen and I. R. McDonald. *Theory of Simple Liquids*. Academic Press, 2006.
- [23] H. Spohn. Nonlinear fluctuating hydrodynamics for anharmonic chains. *J. Stat. Phys.*, 154(5):1191–1227, 2014.
- [24] L. Delfini, S. Denisov, S. Lepri, R. Livi, P. K. Mohanty, and A. Politi. Energy diffusion in hard-point systems. *Eur. Phys. J. Special Topics*, 146(1):21–35, 2007.
- [25] H. Zhao. Identifying diffusion processes in one-dimensional lattices in thermal equilibrium. *Phys. Rev. Lett.*, 96:140602, Apr 2006.